JMB

Altering Molecular Recognition of RNA Aptamers by Allosteric Selection

Garrett A. Soukup, Gail A. M. Emilsson and Ronald R. Breaker*

Department of Molecular Cellular and Developmental Biology, Yale University, New Haven, CT 06520-8103, USA

In a continuing effort to explore structural and functional dynamics in RNA catalysis, we have created a series of allosteric hammerhead ribozymes that are activated by theophylline. Representative ribozymes exhibit greater than 3000-fold activation upon effector-binding and cleave with maximum rate constants that are equivalent to the unmodified hammerhead ribozyme. In addition, we have evolved a variant allosteric ribozyme that exhibits an effector specificity change from theophylline to 3-methylxanthine. Molecular discrimination between the two effectors appears to be mediated by subtle conformational differences that originate from displacement of the phosphodiester backbone near the effector binding pocket. These findings reveal the importance of abstruse aspects of molecular recognition by nucleic acids that are likely to be unapproachable by current methods of rational design.

© 2000 Academic Press

Keywords: aptamer; ribozyme; hammerhead; self-cleavage; molecular switch

*Corresponding author

Introduction

Nucleic acids can form high-affinity ligand-binding sites for a variety of compounds (Chow & Bogdan, 1997; Famulok, 1999). Such ligand binding or "aptamer" motifs typically employ sophisticated structural arrangements, in which the cognate ligand is an integral component of the folded architecture (Feigon *et al.*, 1996; Patel *et al.*, 1997). Detailed analyses of aptamer-ligand complexes have contributed a wealth of information concerning nucleic acid structure and molecular recognition. However, strategies for tailoring the molecular interactions of aptamers rely largely on combinatorial selection techniques (Gold *et al.*, 1995; Osborne & Ellington, 1997) rather than rational design.

While the study of distinct intermolecular interactions can reveal general tactics for the organization of ligand-binding sites (Hermann & Patel, 1999), the investigation of related aptamer complexes is expected to divulge the nuances of molecular recognition. Therefore, related aptamer motifs that bind similar compounds provide an opportunity to examine the precise interactions that dictate ligand binding. For example, related aptamers that selectively bind the compounds arginine or citrulline (Famulok, 1994) differ from each other by only three nucleotides. Structural studies (Yang *et al.*, 1996) of both aptamers reveal that their global structures are similar and that molecular discrimination is achieved mainly through hydrogen bonding interactions between the ligand and the three residues that differ between the aptamers. Thus, a rationale for ligand specificity is apparent if not predictable.

To investigate further the discrete factors that affect molecular recognition, we chose to use an "allosteric selection" strategy (Koizumi *et al.*, 1999) to create new sets of related aptamers. Modular rational design (Tang & Breaker, 1997, 1998; Araki *et al.*, 1998; Soukup & Breaker, 1999a) and *in vitro* selection techniques (Soukup & Breaker, 1999b) have been exploited to develop allosteric ribozymes (Soukup & Breaker, 1999c, 2000) from existing aptamers and catalytic RNAs. Such allosteric ribozymes can be either activated or inhibited by ligand binding to the appended aptamer domain. Here, ligand-dependent catalysts were developed by integrating the theophylline aptamer (Jenison *et al.*, 1994) with the hammerhead ribozyme (Ruffner *et al.*, 1990; Fedor & Uhlenbeck, 1992). Subsequently, one theophylline-dependent ribozyme was subjected to allosteric selection (Koizumi *et al.*, 1999), a process by which the aptamer domain is randomized and allosteric catalysts with new effector specificities are selected in parallel. In

---

Abbreviations used: DMS, dimethyl sulfate; NAIM, nucleotide analog interference mapping.

E-mail address of the corresponding author: ronald.breaker@yale.edu

this manner, we investigated whether related aptamer motifs may exist that are capable of binding any of eight theophylline analogs. A variant allosteric ribozyme was isolated that carries a single mutation, which defines a specificity switch from theophylline to 3-methylxanthine. Both molecular modeling and biochemical analyses of the 3-methylxanthine aptamer suggest that molecular discrimination is accomplished through interactions that would be difficult to envision and to engineer using current rational design strategies.

Results and Discussion

Engineering new theophylline-dependent ribozymes

Allosteric hammerhead ribozymes that are activated by theophylline were isolated from a population of 10^6 RNA molecules, each of which carries the theophylline aptamer (Jenison *et al.*, 1994) and hammerhead ribozyme (Ruffner *et al.*, 1990; Fedor & Uhlenbeck, 1992) motifs adjoined through a random-sequence element (Figure 1(a)). Using an iterative *in vitro* selection technique (Soukup & Breaker, 1999b), populations of theophylline-dependent ribozymes were isolated by selection against self-cleavage in the absence of effector and selection for self-cleavage in the presence of effector. The activity of each population was monitored throughout the selection process to determine the approximate observed rate constant (k_{obs}) for effector-dependent cleavage (Figure 1(b)). After eight

rounds of selection, the population exhibited a theophylline-dependent k_{obs} of ~ 1 min^{-1}. This rate constant is characteristic of an unmodified hammerhead ribozyme (Ruffner *et al.*, 1990), suggesting that individual members of the population had achieved maximal catalytic activity.

The final population (G8) was cloned and five individuals that exhibited superior catalytic parameters were sequenced and further characterized (Table 1). Each member carries a unique bridge sequence or ''communication module'' (Soukup & Breaker, 1999b) that confers unique ligand-sensitivity upon the ribozyme domain. Each ribozyme is activated between 1300 and 4700-fold by theophylline binding under *in vitro* selection conditions, where k_{obs} in the presence of effector (k_{obs}^+) is ~ 1 min^{-1}. These allosteric ribozymes achieve effector-dependent modulation without compromising the maximum possible rate constatn of the ribozyme. In addition, the apparent dissociation constants (apparent K_d) for allosteric ribozymes containing the communication modules cm$^+$theo3 and cm$^+$theo5 were determined (see Materials and Methods). Each ribozyme binds effector with reduced affinity (40 to 100-fold larger K_d) compared to that previously determined for theophylline interaction with the RNA aptamer alone (original K_d of ~ 0.4 μM; Jenison *et al.*, 1994).

When preincubated in reaction buffer, only one ribozyme (containing cm$^+$theo3) demonstrates the ability to convert rapidly from an inactive to an active state upon addition of effector (Table 1). Preliminary results indicate that modest concen-
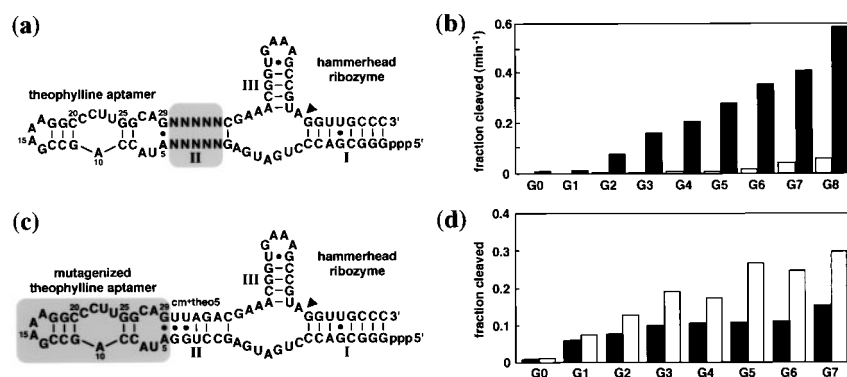

Figure 1. Isolation of theophylline- and analog-dependent ribozymes. (a) Initial population for *in vitro* selection of ribozymes that are activated by theophylline. Each molecule carries the conserved cores of the theophylline aptamer and the hammerhead ribozyme joined through a stem II element comprised of random-sequence nucleotides (shaded). Roman numerals denote the stem elements of the hammerhead motif. The site of self-cleavage is indicated (arrowhead). Nucleotides comprising the theophylline aptamer are numbered according to Zimmermann *et al.* (1997). (b) Theophylline-dependent ribozymes were derived by conducting eight rounds of selection, each consisting of selection against ligand-independent activity followed by selection for ligand-dependent cleavage (see Materials and Methods). Plotted are the activities of the initial population (G0) and subsequent populations (G1-G8) in the absence (open bars) and presence (filled bars) of 200 μM theophylline. Activity is represented as the fraction of each population cleaved normalized with respect to reaction time. Note that G8 cleavage corresponds to a k_{obs} value of ~ 1 min^{-1}, which is the maximum k_{obs} for the unmodified hammerhead ribozyme. (c) Initial population for altering effector specificity by allosteric selection. The initial population is derivative of the theophylline-dependent ribozyme containing cm$^+$theo5 (Table 1). The 25 nt core of the theophylline aptamer (shaded) was mutagenized with a degeneracy of 0.18 per position (Breaker & Joyce, 1994). (d) Allosteric selection for altered ligand binding specificity. Populations of ribozymes were first selected against theophylline-activation and subsequently selected for cleavage in the presence of eight theophylline analogs (see Table 2). The activity of each population in a solution containing 200 μM theophylline (filled bars) or 200 μM of each theophylline analog (open bars) is represented as the fraction of the population cleaved in one minute (G0-G3, G5-G7) or 30 seconds (G4).

trations (50 mM) of Tris or Hepes prevent rapid switching of the ribozyme containing cm+theo2 (data not shown). The theophylline-dependent activity of certain ribozymes therefore is contingent upon the presence or concentration of other solutes in the reaction. In addition, the ability of each communication module to confer general effector-dependence upon the hammerhead ribozyme was examined by replacing the theophylline aptamer domain with a different aptamer sequence that binds FMN (Burgstaller & Famulok, 1994; Fan *et al.*, 1996). Both cm+theo4 and cm+theo5 were found to mediate FMN-dependent activation (Table 1), demonstrating that their function is not highly dependent upon the neighboring sequence or ligand specificity of the appended aptamer domain. These results and those reported previously (Soukup & Breaker, 1999b) demonstrate that new allosteric ribozymes can be engineered simply by interchanging aptamer domains.

To investigate whether an integrated aptamer-ribozyme construct exhibits similar ligand specificity and affinity as does the independent aptamer, a comparison was made between the theophylline aptamer and the ribozyme containing cm+theo3 (Table 2). The relative activity of the ribozyme in the presence of theophylline *versus* related compounds was found to be comparable to the relative K_d of the aptamer alone (Jenison *et al.*, 1994). Given this correlation, it is likely that the effector-modulated catalytic activity of allosteric ribozymes accurately reflects ligand binding affinity. Furthermore, these data demonstrate that the basic properties of the theophylline aptamer persist in different contexts and when applied toward novel functionality.

Altering the effector specificity of an allosteric ribozyme

A population of molecules based on the theophylline-dependent ribozyme containing cm+theo5 (Figure 1(c)) was subjected to allosteric selection (Koizumi *et al.*, 1999) in order to address whether variants of the theophylline aptamer can be created that specifically recognize related compounds. Allosteric ribozymes with altered effector specificity were developed by selection against self-cleavage in the presence of theophylline followed by selection for self-cleavage in a solution containing the eight theophylline analogs listed in Table 2. Analog-responsive populations of ribozymes were quickly isolated using this strategy (Figure 1(d)). However, each population exhibits only a modest enhancement in self-cleavage in the presence of the analog mixture even after seven rounds of selection. This final population (G7) was cloned and individuals were screened for analog-dependent activity.

A detailed analysis was conducted on one variant ribozyme that was isolated from the G7 population. This prototypic 3-methylxanthine-dependent ribozyme carries three mutations relative to the theophylline-dependent ribozyme (Figure 2(a)), each of which resides within the ligand-binding domain. The C to A mutation at position 27 (C27A) is not expected to contribute to the altered ligand binding specificity. First, this

Table 1. Sequences, kinetic parameters, and attributes of communication modules for theophylline-dependent ribozymes

Module[a]	Sequence	k_{obs}^- (min^{-1})[b]	k_{obs}^+ (min^{-1})[c]	Fold activation[d]	Apparent K_d (μM)	Rapid switching[f]	Domain swapping[g]
cm+theo1	5'-AUUGA GGACC-5'	3.3×10^{-4}	1.1	3300	nd[e]	−	−
cm+theo2	UUUGA GAACC	1.9×10^{-4}	9.0×10^{-1}	4700	nd	−	−
cm+theo3	UCUUA GGUCU	4.1×10^{-4}	5.2×10^{-1}	1300	~15	+	−
cm+theo4	UCAUA GGUCC	2.7×10^{-4}	9.0×10^{-1}	3300	nd	−	+
cm+theo5	UUAGA GGUCC	6.2×10^{-4}	1.4	2300	~40	−	+

[a] The designation for each communication module (cm) conveys that allosteric activation ($^+$) was originally acheived with an effector specificity for theophylline (theo), and provides an arabic numeral for the sequence class of module in the series (Koizumi *et al.*, 1999).
[b] Observed rate constant for self-cleavage in the absence of theophylline (k_{obs}^-).
[c] Initial observed rate constant for self-cleavage in the presence of 200 μM theophylline (k_{obs}^+).
[d] k_{obs}^+/k_{obs}^-.
[e] Not determined.
[f] Denotes the ability of the theophylline-dependent ribozyme to rapidly convert (Soukup & Breaker, 1999b) to the active form upon addition of 200 μM theophylline to a preincubated mixture containing 50 mM Tris-HCl (pH 7.5 at 23 °C), 20 mM MgCl$_2$, and ^{32}P-labeled RNA.
[g] Denotes the ability of the communication module to confer ligand-dependent activity to a hammerhead ribozyme when the theophylline aptamer is replaced with an FMN aptamer (Soukup & Breaker, 1999b).
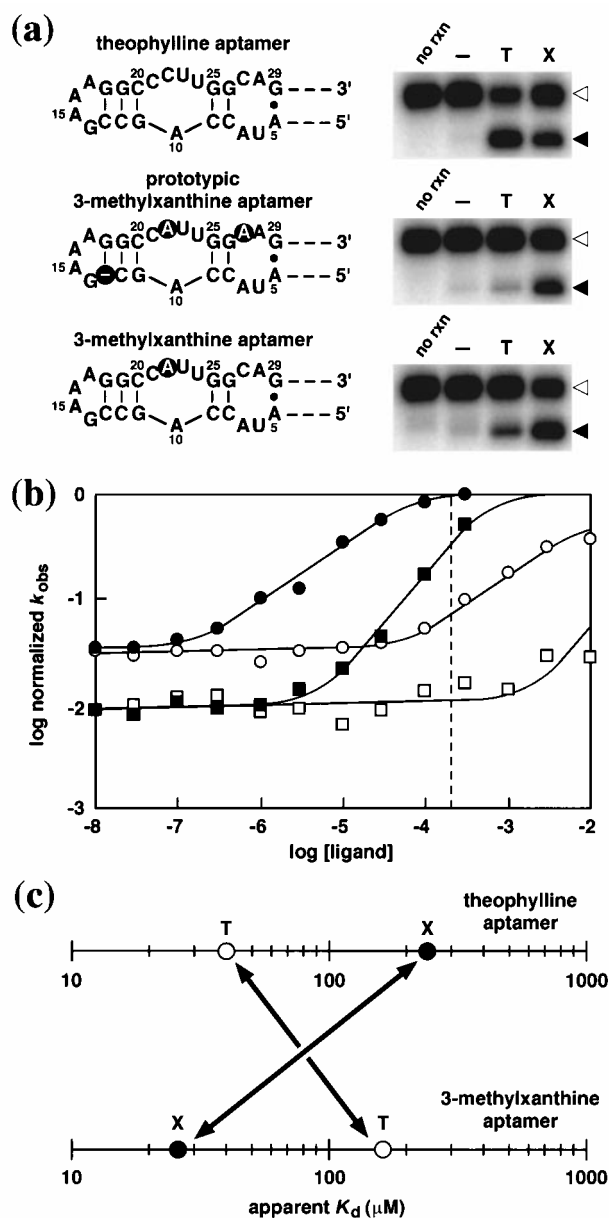
Figure 2. Comparison of theophylline- and 3-methylxanthine-dependent ribozymes containing cm+theo5. (a) Sequences and activities of ligand-dependent ribozymes. Shown are the aptamer domains of the theophylline-, prototypic 3-methylxanthine-, and 3-methylxanthine-dependent ribozymes (arranged from top to bottom). The prototypic 3-methylxanthine aptamer carries three mutations (encircled) relative to the theophylline aptamer, whereas the 3-methylxanthine aptamer contains only the C22A mutation. The cleavage activity under selection conditions is shown to the right of each corresponding construct. Ribozymes were reacted in the absence (−) or presence of 200 μM theophylline (T) or 200 μM 3-methylxanthine (X) for one minute and were subsequently separated by denaturing 10 % PAGE. For each construct, a control (no rxn) was prepared with unreacted ribozyme. Open and filled arrowheads denote uncleaved and cleaved RNA, respectively. (b) Ligand-dependent activities of 3-methylxanthine-dependent ribozymes. The logarithm of the k_{obs} (normalized to the maximum k_{obs}) *versus* the logarithm of the molar ligand concentration is plotted for the prototypic 3-methylxanthine-dependent ribozyme (squares) and the 3-methylxanthine-dependent ribozyme (circles) in the presence of theophylline (open symbols) or 3-methylxanthine (filled symbols). The broken line indicates the concentration of each ligand (200 μM) used during allosteric preselection and selection. (c) Apparent dissociation constants for binding of ligands to the theophylline- and 3-methylxanthine-dependent ribozymes. The apparent K_d values for theophylline (open circle) or 3-methylxanthine (filled circle) are plotted for each ribozyme on a logarithmic scale. The arrows illustrate the inversion of effector specificities for the ribozymes.

mutation has previously been characterized in the theophylline aptamer (Jenison *et al.*, 1994), and does not affect ligand binding. Second, the base at this position is bulged outward from the core of the ligand-bound structure (Zimmermann *et al.*, 1997, 1998). In a similar fashion, deletion of C13 also is not expected to affect ligand binding, since this base resides in a stem-loop region whose sequence is not conserved. However, the identity of the nucleotide at position 22 is expected to greatly impact molecular recognition, since C22 is modeled to interact directly with ligand in the structure of the theophylline aptamer (Zimmermann *et al.*, 1997). To assess the contri-

bution that this mutation makes to effector binding specificity, a variant with a single C22A mutation was examined. Indeed, we find that the C22A mutation alone is sufficient to account for the change in ligand-binding specificity between the theophylline- and 3-methylxanthine-dependent ribozymes (Figure 2(a)).

It is surprising that none of the individual ribozymes characterized from G7 carry the single C22A mutation in isolation (data not shown) despite the fact that this variant should have been well represented in the initial population (~1 copy for every 2000 molecules). A possible rationale for this occurrence is provided by a detailed compari-

Table 2. Dissociation constants for ligand binding to the theophylline aptamer as compared to the ligand-dependent activities of allosteric hammerhead ribozymes

Ligand	Relative K_d theophylline aptamer[a]	Relative k_{obs} theophylline aptamer[b]	Relative k_{obs} 3-methylxanthine aptamer[c]
Theophylline	1.0	1.0	6.3
Xanthine	27	105	2.3
1-Methylxanthine	28	53	>73[d]
3-Methylxanthine	6.3	18	1.0
7-Methylxanthine	>1500	>380[d]	8.8
3,7-Dimethylxanthine	>1500	>380	8.0
1,3-Dimethyluric acid	>3100	>380	>73
Hypoxanthine	153	129	>73
Caffeine	10,900	>380	>73

[a] Relative dissociation constant (K_d) is the ratio of K_d(c) for ligand binding to K_d(t) for theophylline binding as previously determined (Jenison *et al.*, 1994).
[b] Relative observed rate constant (k_{obs}) is the ratio of k_{obs} in the presence of theophylline to k_{obs} in the presence of ligand, where each ligand is at a concentration equal to the apparent K_d (15 μM) for theophylline interaction with the allosteric ribozyme containing cm$^+$theo3 and the theophylline aptamer.
[c] Relative observed rate constant (k_{obs}) is the ratio of k_{obs} in the presence of 3-methylxanthine to k_{obs} in the presence of ligand, where each ligand is at a concentration equal to the apparent K_d (25 μM) for 3-methylxanthine interaction with the allosteric ribozyme containing cm$^+$theo5 and the 3-methylxanthine aptamer.
[d] k_{obs} in the presence of ligand was not detectably higher than that in the absence of ligand.

son of the 3-methylxanthine-dependent ribozyme and its prototype (Figure 2(b)). The prototypic 3-methylxanthine-dependent ribozyme has a lower background rate of cleavage, and its apparent affinity for both theophylline and 3-methylxanthine is weakened. These kinetic properties allowed the prototype to resist negative selection more effectively than the related single-nucleotide variant. Therefore, the relatively impaired prototype has a distinct advantage over the single-nucleotide variant during allosteric selection. These results demonstrate that ligand concentration can significantly impact the kinetic properties of successful ribozymes in allosteric selection.

The theophylline- and 3-methylxanthine-dependent ribozymes exhibit inverted effector-binding specificities and affinities (Figure 2(c)). Since theophylline (i.e. 1,3-dimethylxanthine) and 3-methylxanthine differ only by a methyl substituent at the N1 position, the 3-methylxanthine-dependent ribozyme is expected to most strongly discriminate against derivatives of 1-methylxanthine. A more detailed analysis of the 3-methylxanthine-dependent ribozyme demonstrates that 1-methylxanthine, caffeine (i.e. 1,3,7-trimethylxanthine), and 1,3-dimethyluric acid are among the compounds with the lowest binding affinities, while xanthine, 3-methylxanthine, 7-methylxanthine, and 3,7-dimethylxanthine are among the compounds with the highest binding affinities (Table 2). These findings indicate that A22 of the 3-methylxanthine aptamer provides an additional ligand-recognition contact that primarily distinguishes xanthine derivatives based on N1 methyl substitution.

A model for 3-methylxanthine recognition

Molecular recognition by the theophylline aptamer is mediated by a number of interdependent tertiary interactions (Zimmermann *et al.*, 1997). Within the core of the aptamer motif, theophylline participates in one of three consecutive base-triple interactions, where both stacking and hydrogen bonding contribute to the overall stability of the complex. Molecular discrimination appears to be most influenced by interaction of the ligand with C22 and U24 in the central base-triplet (Figure 3(a)). The array of hydrogen bonds that orient the ligand in the binding site provide a rationale for the ability of the aptamer to distinguish theophylline from closely related compounds such as caffeine (Jenison *et al.*, 1994; Zimmermann *et al.*, 1997). Since C22 and U24 define theophylline recognition, the corresponding A22 and U24 nucleotides in the 3-methylxanthine aptamer might define its altered binding specificity.

We speculated that the C22A mutation does not alter the general fold of the 3-methylxanthine aptamer relative to the theophylline aptamer. If true, then A22 could substitute for C22 in the 3-methylxanthine aptamer by forming similar hydrogen bonding interactions with the ligand. However, ligand binding could be mediated by A22 in either *syn* (Figure 3(b)) or *anti* (Figure 3(c)) conformation. Interaction of ligand with the exocyclic amine (N6) and N7 of A22 in *syn* conformation could conceivably occur without disruption of the overall aptamer structure (Figure 3(b)). Consequently, this conformation of the ligand binding pocket does not provide a clear mechanism for altering the specificity of the 3-methylxanthine aptamer. Alternatively, interaction of ligand with N6 and N1 of A22 in *anti* conformation would require a 3 to 4 Å displacement of the phosphodiester backbone (Figure 3(c) and (d)). Therefore, subtle conformational changes that originate from displacement of the backbone by A22 in *anti* conformation might account for the altered ligand binding specificity of
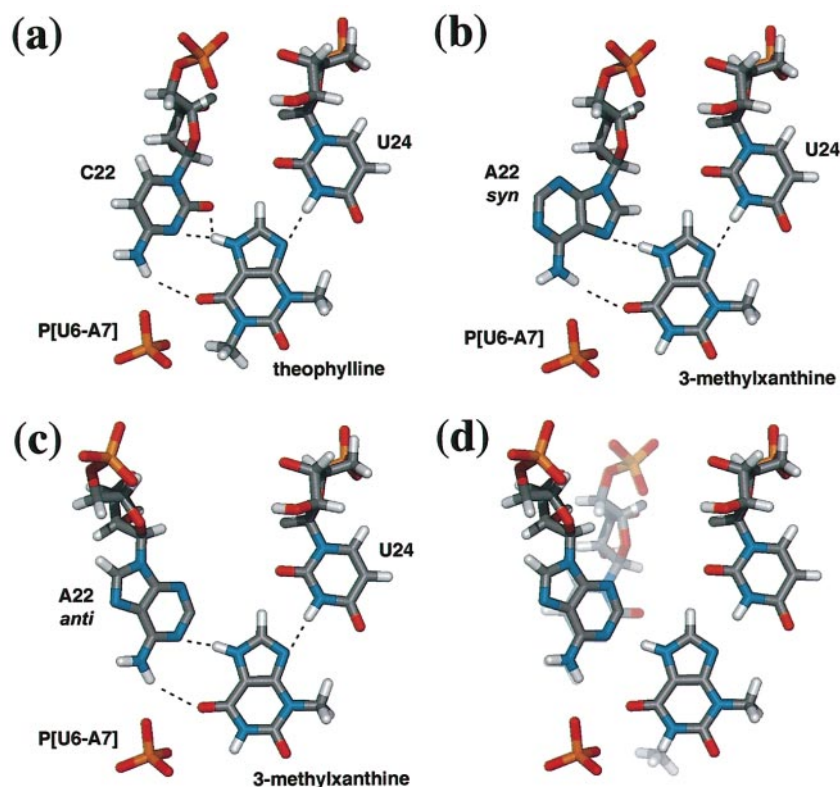
Figure 3. Models of ligand-aptamer interactions. (a) Base-triple interaction involving theophylline, C22, and U24 from the structure of the theophylline-binding aptamer reported by Zimmermann *et al.* (1997). The phosphate moiety bridging nucleotides U6 and A7 (P(U6-A7)) traverses the plane of the base-triple immediately adjacent to the N1 methyl group of theophylline. Atoms that comprise the xanthine ring of the ligand are numbered according to the convention for a purine base. Broken lines represent proposed hydrogen bonds. Carbon (gray); hydrogen (white); nitrogen (blue); oxygen (red); and phosphorus (orange) atoms are depicted. (b) Model for 3-methylxanthine recognition mediated by A22 in *syn* conformation. A22 substitutes for C22 of the theophylline aptamer without displacement of the phosphodiester backbone. (c) Model for 3-methylxanthine recognition mediated by A22 in *anti* conformation. A22 substitutes for C22 with a 3-4 Å displacement of the phosphodiester backbone. (d) Superimposition of the theophylline- and 3-methylxanthine-binding models depicted in (a) and (c) revealing the displacement of the phosphodiester backbone by A22 in *anti* conformation.

the 3-methylxanthine aptamer. Barring massive rearrangement of the aptamer, the only candidate structure that could mediate molecular discrimination against the N1 methyl group of theophylline is the phosphate that bridges the U6 and A7 nucleotides. In the theophylline aptamer, this phosphodiester linkage traverses the plane of the C22·ligand·U24 base-triplet immediately adjacent to the N1 position of the ligand.

In order to assess which conformation of A22 is relevant to 3-methylxanthine recognition, the 3-methylxanthine-dependent ribozyme was examined using nucleotide analog interference mapping (NAIM; Strobel, 1999; Ryder & Strobel, 1999) and chemical probing techniques (Krol & Carbon, 1989). NAIM makes use of phosphorothioate-labeled nucleotide analogs to identify functional groups that are important for RNA activity. Analysis of the 3-methylxanthine-dependent ribozyme using adenosine analogs that replace N7 with carbon (7-deaza-adenosine 5′-thiophosphate; 7dAαS) or that replace N6 with hydrogen (purine ribonucleoside 5′-thiophosphate; PurαS) reveals the importance of these functional groups at certain positions for effector binding and allosteric activation of ribozyme activity (Figure 4(a)). We find that only the N6 position and not the N7 position of A22 is important for allosteric function of the 3-methylxanthine-dependent ribozyme. In

addition, chemical modification of each adenosine at the N1 position by dimethyl sulfate (DMS) was used to probe the effector-bound conformation of the 3-methylxanthine-dependent ribozyme (Figure 4(b)). In this case, we find that bound effector protects N1 of A22 from methylation by DMS. Therefore, both interference mapping and chemical modification of the 3-methylxanthine aptamer motif support a model of ligand recognition by A22 in *anti* conformation (Figure 3(c)) if the global structure of the original aptamer is retained.

The overall structural fold of the 3-methylxanthine aptamer was assessed using the same biochemical analyses described above. The patterns of modification interference and protection observed for the 3-methylxanthine-dependent ribozyme are consistent with the structural model of the theophylline aptamer (Zimmermann *et al.*, 1997), which indicates a conservation of the structural fold between the two aptamers. For example, N6 or N7 modification of A15, A16, or A17 does not interfere with effector binding or allosteric activation (Figure 4(a), lanes 6 and 9). In addition, each nucleotide is susceptible to N1 modification by DMS in the absence or presence of effector (Figure 4(b), compare lanes 3 and 4). These results are consistent with the neutral role of each nucleotide in the tetraloop structure of the aptamer motif. Conversely, A5·G29 pairing and U6·A28·U23 tri-
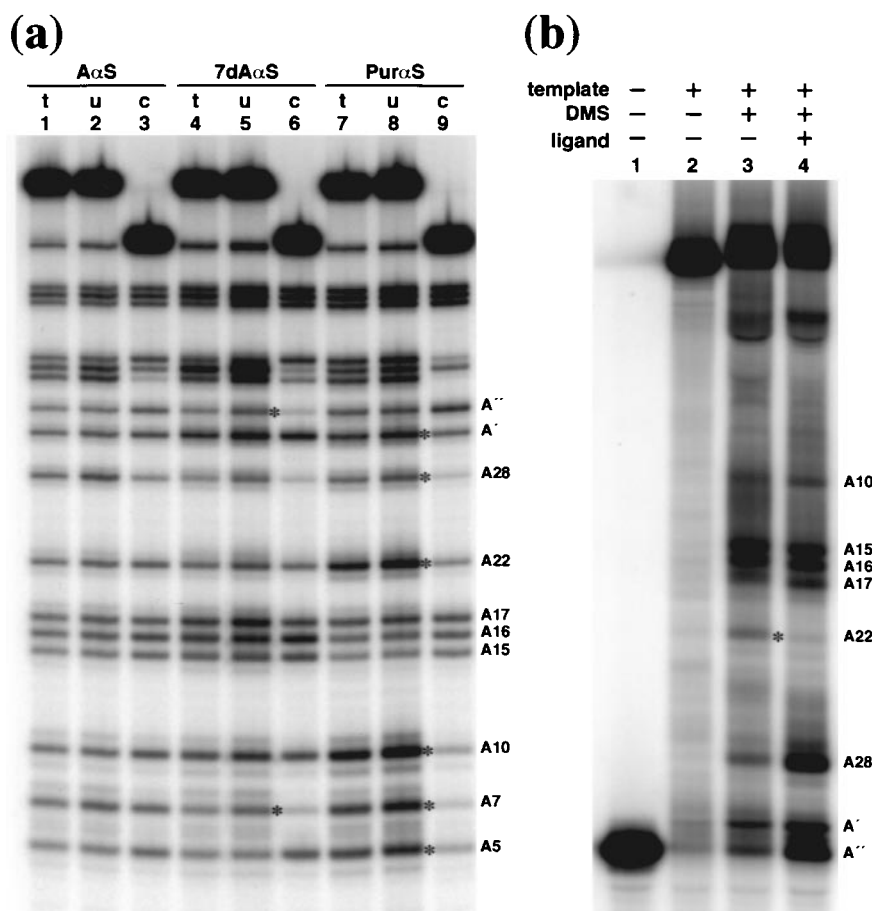
Figure 4. Identification of chemical groups involved in ligand binding to the 3-methylxanthine-dependent ribozyme. (a) NAIM of the 3-methylxanthine-dependent ribozyme. The positions of phosphorothioate nucleotide analogs incorporated in 3-methylxanthine-dependent ribozymes ((5′-^{32}P)-labeled) are detected by iodine-mediated cleavage and separation by denaturing 10 % PAGE. For each analog examined, iodine-mediated cleavage patterns are shown for the transcript (t), and for the uncleaved ribozymes (u) and cleaved ribozymes (c) purified after reaction in the presence of 3-methylxanthine at a concentration equivalent to the apparent K_d (25 μM) of the effector. Phosphorothioate nucleotide analogs of adenosine (AαS) examined are 7-deaza-adenosine (7dAαS) and purine ribonucleoside (PurαS). Positions at which substitution by the analog interfere with function of the ribozyme appear as gaps in the iodine-mediated cleavage pattern of the self-processed (active) ribozymes relative to the transcripts. Interference κ values for each site denoted by an asterisk reflect the fold difference in activity relative to the parent analog (AαS). κ values are 2.6 (A7) and 4.0 (A″) for 7dAαS, and 8.4 (A5), 15 (A7), 11 (A10), 5.9 (A22), 2.5 (A28), and 2.3 (A′) for PurαS. A′ and A″ denote, respectively, the 5′ and 3′ adenosine residues of cm⁺theo5 (Table 1). Interference resulting from modification of A7 or A10 is not predicted by hydrogen bonding interactions in the structural model of the theophylline aptamer motif and could reflect the affect of these modifications on RNA folding. (b) Chemical probing of the 3-methylxanthine-dependent ribozyme. Methylation of adenosine residues at the N1 position by dimethyl sulfate (DMS) blocks reverse transcription of modified templates. Reverse transcription products derived from (5′-^{32}P)-labeled primer are separated by denaturing 10 % PAGE. Templates for each reaction were prepared by incubation in the absence (lane 2) or presence (lane 3) of DMS under semi-denaturing conditions, or incubation in the presence of DMS and a saturating amount of 3-methylxanthine (250 μM) under native conditions (lane 4). The asterisk denotes the site of protection from DMS modification at the N1 position of nucleotide A22 in the effector-bound ribozyme. Note that reverse transcription products derived from templates carrying modifications 5′ to nucleotide A10 are not well resolved.

plet formation are two of the primary interactions that establish the core of the theophylline aptamer. If pairing between nucleotides A5 and G29 is retained in the 3-methylxanthine aptamer, then interference of ribozyme activity will result from modification of the N6 position of A5. In a similar fashion, if pairing of A28 and U23 in the U6·A28·U23 triplet is retained, then modification

of the N6 or N7 position of A28 will interfere with ribozyme activity, while N1 modification by DMS should be permissible. Indeed, three of these four putative contacts are supported by data derived from interference mapping and chemical modification of the 3-methylxanthine-dependent ribozyme. Specifically, N6 modification of A5 or A28 interferes with ligand-dependent ribozyme activity

(Figure 4(a), lane 9), and the N1 position of A28 is accessible to modification by DMS in the ligand-bound ribozyme (Figure 4(b), compare lanes 3 and 4). However, no significant interference is observed to result from N7 modification of A28 in addition to the observed phosphorothioate effect (Figure 4(a), lane 6; see also Materials and Methods). The lack of predicted interference at A28 due to N7 modification does not negate the role of the nucleotide in U6·A28·U23 triplet formation. Perhaps, disruption of this particular hydrogen bond has a negligible affect on the stability of the base-triplet. Taken together, these data are consistent with a general structural fold for the 3-methyl-xanthine aptamer that is similar to the original structure of the theophylline aptamer, but support a new mode of molecular recognition by A22 in *anti* conformation. Additional study will be required to elucidate the molecular basis for discrimination by the 3-methylxanthine aptamer.

Interestingly, the affect of functional group modification on the performance of the communication module is also observed. N6 modification of the 5′ adenosine (A′) and N7 modification of the 3′ adenosine (A″) both interfere with the function of cm$^+$theo5 (Figure 4(a), lanes 6 and 9). The former is consistent with the base-pairing scheme proposed for the active state of cm$^+$theo5 (Figure 1(c)). The latter suggests that A″ might be involved in an unusual interaction that is necessary for allosteric activation of the ribozyme. However, these experiments do not reveal whether these modifications interfere with the active structure, the inactive structure, or the transition between the two. Although the interference patterns are consistent with the ''slip-structure'' mechanism originally proposed (Soukup & Breaker, 1999b), more extensive analyses are required to confirm the precise mechanism of allosteric transition.

This study demonstrates that related aptamer motifs with new ligand specificities can be developed by allosteric selection. This strategy not only provides a rapid method for the simultaneous development of novel intermolecular interactions, but also provides a means of examining the details of nucleic acid structure and molecular recognition. Additional sets of related aptamers, like the theophylline and 3-methylxanthine pair, could be generated to serve as model compounds for the study of molecular recognition by nucleic acids. Our findings also serve to illustrate aspects of molecular recognition that are currently difficult to address using only rational design strategies. At present, engineering ligand or substrate specificity of nucleic acids typically involves altering hydrogen bond donor and acceptor pairs (e.g. Michel *et al.*, 1989). However, other aspects of folding can play a significant role in molecular recognition and these interactions are not easily predicted or manipulated. Most likely, an intersection of rational design and combinatorial techniques will continue to be the best strategy for developing functional nucleic acids with atomic-scale specifications.

Materials and Methods

In vitro selection

In vitro selection for theophylline-dependent ribozymes was performed as previously described (Soukup & Breaker, 1999b). RNA populations (10^{12}-10^{13} molecules; 0.8-1.6 μM) were preselected against ligand-independent cleavage in reaction buffer (50 mM Tris-HCl (pH 7.5 at 23 °C), 20 mM MgCl$_2$) by incubation for five hours at 25 °C punctuated at one hour intervals by incubation at 60 °C for one minute. The uncleaved fraction of each population was purified by denaturing 10 % polyacrylamide gel electrophoresis (PAGE) and subsequently selected for cleavage in the presence of 200 μM theophylline in reaction buffer by incubation at 23 °C for 30 seconds to five minutes.

Allosteric selection for theophylline analog-dependent ribozymes was similarly performed. RNA populations (10^{13}-10^{14} molecules; 1.6-10 μM) were preselected against theophylline-dependent cleavage in reaction buffer containing 200 μM theophylline by incubation for 2.5 hours at 25 °C punctuated at 30 minute intervals by incubation at 90 °C for 30 seconds. Following purification of the uncleaved fraction by denaturing PAGE, populations G2-G4 were subjected to a second preselection and purification step. Preselection of populations G5-G7 was performed by using four iterations of preselection in the presence of theophylline for 30 minutes at 23 °C, precipitation with ethanol, denaturation by brief incubation with mild alkali, neutralization, and precipitation with ethanol (Koizumi *et al.*, 1999). Following purification by denaturing 10 % PAGE, the uncleaved fraction of each population was selected for cleavage in reaction buffer containing 200 μM of each of the eight theophylline analogs (Table 2) for one minute (G0-G3; G5-G7) or 30 seconds (G4) at 23 °C.

Characterization of allosteric ribozymes

Individual molecules were isolated from the final population of each selection by cloning (TOPO TA Cloning Kit, Invitrogen) and analyzed by sequencing (ThermalSequenase Kit, Amersham). RNAs were prepared by *in vitro* transcription using T7 RNA polymerase (Soukup & Breaker, 1999a) and double-stranded DNA templates derived from each clone by PCR amplification (Soukup & Breaker, 1999b) or from synthetic DNAs by primer extension using reverse transcriptase (Soukup & Breaker, 1999a). Self-cleavage reactions containing internally ^{32}P-labeled or (5′-^{32}P)-labeled RNA (1 to 500 nM) and ligand (10 nM to 10 mM), where ligand concentration was at least tenfold greater than ribozyme concentration, were initiated by the addition of reaction buffer unless otherwise indicated. Cleavage products were separated by denaturing 10 % PAGE, and examined using a PhosphorImager and ImageQuaNT software (Molecular Dynamics). Observed rate constants (k_{obs}) were derived by plotting the natural logarithm of the fraction of uncleaved RNA versus time and establishing the negative slope of the resulting line. Apparent dissociation constants (K_d) were established as the concentration of ligand required to produce 1/2 maximum k_{obs} (Soukup & Breaker, 1999b). Alternatively, the apparent K_d for ligand interaction was derived using the following equation:

$$K_{\mathrm{d}}^{x} = K_{\mathrm{d}}^{y}\left(\frac{k_{\mathrm{obs}}^{y}}{k_{\mathrm{obs}}^{x}}\right)$$

where K_{d}^{x} and K_{d}^{y} are, respectively, the apparent dissociation constants for binding to compounds x and y, where compound y has the higher affinity. k_{obs}^{x} and k_{obs}^{y} are, respectively, the observed rate constants for self-cleavage in the presence of compounds x and y at a concentration equal to K_{d}^{y}. The ratio of k_{obs}^{y} and k_{obs}^{x} provide the relative k_{obs} reported in Table 2.

Molecular modeling

Molecular graphics images were produced on a Silicon Graphics workstation using MidasPlus (Ferrin *et al.*, 1988) from the Computer Graphics Laboratory, University of California, San Francisco. Each model was derived by partial rendition of model 1 of the theophylline aptamer structure (Zimmermann *et al.*, 1997). For each model, base planarity and the position of potential hydrogen bond donors and acceptors are conserved at nucleotide position 22.

Nucleotide analog interference mapping (NAIM)

Nucleotide analogs for NAIM were the generous gift of S.A. Strobel. Each analog was randomly incorporated into RNA at a frequency of 0.05 per position by transcription using T7 RNA polymerase as described (Ryder & Strobel, 1999). RNA was dephosphorylated, (5′-^{32}P)-labeled, and purified by denaturing 10 % PAGE. Labeled transcripts were incubated in reaction buffer for 30 seconds at 23 °C in the presence of 3-methylxanthine at a concentration equivalent to the K_{d} (25 μM) of the effector. Reaction under these conditions results in <50 % cleavage of RNA transcripts. The uncleaved and cleaved fractions of RNA were separated and purified by denaturing 10 % PAGE. Phosphorothioate linkages in RNA transcripts were cleaved by treatment with iodine (Gish & Eckstein, 1988) and the products were resolved by denaturing 10 % PAGE. Interference κ values were derived as described (Ortoleva-Donnelly *et al.*, 1998) and are considered to represent a significant level of interference when greater than a value of 2.

Chemical modification

RNA (~30 pmol) was incubated for 30 minutes at 23 °C in the absence or presence of DMS (~10 μmol) under semi-denaturing conditions (50 mM Hepes (pH 7.4 at 23 °C), 1 mM EDTA), or in the presence of DMS and 250 μM 3-methylxanthine under native conditions (50 mM Hepes (pH 7.4 at 23 °C), 20 mM MgCl$_2$). Reactions were terminated by the addition of 2-mercaptoethanol (~40 μmol) and RNA was precipitated with ethanol. RNA was reverse transcribed using (5′-^{32}P)-labeled primer (5′-GGGCAACCTACGGCTTTCACCGTTTCG) and the products were separated by denaturing 10 % PAGE. Reverse transcription reactions (10 μl) containing ~3 pmol RNA, ~100 fmol primer, 50 mM Tris-HCl (pH 8.3 at 23 °C), 75 mM KCl, 3 mM MgCl$_2$, 200 μM each dNTP, and 100 units SuperScript II reverse transcriptase (Gibco BRL) were incubated at 37 °C for 30 minutes.

References

Araki, M., Okuno, Y., Hara, Y. & Sugiura, Y. (1998). Allosteric regulation of a ribozyme activity through ligand-induced conformation change. *Nucl. Acids Res.* **26**, 3379-3384.

Breaker, R. R. & Joyce, G. F. (1994). Inventing and improving ribozyme function: rational design versus iterative selection methods. *Trends Biotechnol.* **12**, 268-275.

Burgstaller, P. & Famulok, M. (1994). Isolation of RNA aptamers for biological cofactors by *in vitro* selection. *Angew. Chem. Int. Ed. Engl.* **33**, 1084-1087.

Chow, C. S. & Bogdan, F. M. (1997). A structural basis for RNA-ligand interactions. *Chem. Rev.* **97**, 1489-1513.

Famulok, M. (1994). Molecular recognition of amino acids by RNA-aptamers: an L-citrulline binding RNA motif and its evolution into an L-arginine binder. *J. Am. Chem. Soc.* **116**, 1698-1706.

Famulok, M. (1999). Oligonucleotide aptamers that recognize small molecules. *Curr. Opin. Struct. Biol.* **9**, 324-329.

Fan, P., Suri, A. K., Fiala, R., Live, D. & Patel, D. J. (1996). Molecular recognition in the FMN-RNA aptamer complex. *J. Mol. Biol.* **258**, 480-500.

Fedor, M. J. & Uhlenbeck, O. C. (1992). Kinetics of inter-molecular cleavage by hammerhead ribozymes. *Biochemistry,* **31**, 12042-12054.

Feigon, J., Dieckmann, T. & Smith, F. W. (1996). Aptamer structures from A to ζ. *Chem. Biol.* **3**, 611-617.

Ferrin, T. E., Huang, C. C., Jarvis, L. E. & Langridge, R. (1988). The MIDAS display system. *J. Mol. Graph.* **6**, 13-27.

Gish, G. & Eckstein, F. (1988). DNA and RNA sequence determination based on phosphorothioate chemistry. *Science,* **240**, 1520-1522.

Gold, L., Polinsky, B., Uhlenbeck, O. C. & Yarus, M. (1995). Diversity of oligonucleotide functions. *Annu. Rev. Biochem.* **64**, 763-797.

Hermann, T. & Patel, D. J. (1999). Stitching together RNA tertiary architectures. *J. Mol. Biol.* **294**, 829-849.

Jenison, R. D., Gill, S. C., Pardi, A. & Polisky, B. (1994). High resolution molecular discrimination by RNA. *Science,* **263**, 1425-1429.

Koizumi, M., Soukup, G. A., Kerr, J. N. Q. & Breaker, R. R. (1999). Allosteric selection of ribozymes that respond to the second messengers cGMP and cAMP. *Nature Struct. Biol.* **6**, 1062-1071.

Krol, A. & Carbon, P. (1989). A guide for probing native small nuclear RNA and ribonucleoprotein structures. *Methods Enzymol.* **180**, 212-227.

Michel, F., Hanna, M., Green, R., Bartel, D. P. & Szostak, J. W. (1989). The guanosine binding site of the *Tetrahymena* ribozyme. *Nature,* **342**, 391-395.

Ortoleva-Donnelly, L., Szewczak, A. A., Gutell, R. R. & Strobel, S. A. (1998). The chemical basis of adensine conservation throughout the *Tetrahymena* ribozyme. *RNA,* **4**, 498-519.

Osborne, S. E. & Ellington, A. D. (1997). Nucleic acid selection and the challenge of combinatorial chemistry. *Chem. Rev.* **97**, 349-370.

Patel, D. J., Suri, A. K., Jiang, F., Jiang, L., Fan, P., Kumar, R. A. & Nonin, S. (1997). Structure, recognition and adaptive binding in RNA aptamer complexes. *J. Mol. Biol.* **272**, 645-664.

Ruffner, D. E., Stormo, G. D. & Uhlenbeck, O. C. (1990). Sequence requirements of the hammerhead RNA self-cleavage reaction. *Biochemistry,* **29**, 10695-10702.

Ryder, S. P. & Strobel, S. A. (1999). Nucleotide analog interference mapping. *Methods,* **18**, 38-50.

Soukup, G. A. & Breaker, R. R. (1999a). Design of allosteric hammerhead ribozymes activated by ligand-induced structure stabilization. *Structure,* **7**, 783-791.

Soukup, G. A. & Breaker, R. R. (1999b). Engineering precision RNA molecular switches. *Proc. Natl Acad. Sci. USA,* **96**, 3584-3589.

Soukup, G. A. & Breaker, R. R. (1999c). Nucleic acid molecular switches. *Trends Biotechnol.* **17**, 469-476.

Soukup, G. A. & Breaker, R. R. (2000). Allosteric ribozymes. In *Ribozymes: Biology and Biotechnology* (Gaur, R. K. & Krupp, G., eds), Eaton Publishing, Natick, MA In the press.

Strobel, S. A. (1999). A chemogenetic approach to RNA function/structure analysis. *Curr. Opin. Struct. Biol.* **9**, 346-352.

Tang, J. & Breaker, R. R. (1997). Rational design of allosteric ribozymes. *Chem. Biol.* **4**, 453-459.

Tang, J. & Breaker, R. R. (1998). Mechanism for allosteric inhibition of an ATP-sensitive ribozyme. *Nucl. Acids Res.* **26**, 4222-4229.

Yang, Y., Kochoyan, M., Burgstaller, P., Westhoff, E. & Famulok, M. (1996). Structural basis of ligand discrimination by two related RNA aptamers resolved by NMR spectroscopy. *Science,* **272**, 1343-1347.

Zimmermann, G. R., Jenison, R. D., Wick, C. L., Simorre, J. P. & Pardi, A. (1997). Interlocking structural motifs mediate molecular discrimination by a theophylline-binding RNA. *Nature Struct. Biol.* **4**, 644-649.

Zimmermann, G. R., Shields, T. P., Jenison, R. D., Wick, C. L. & Pardi, A. (1998). A semiconserved residue inhibits complex formation by stabilizing interactions in the free state of a theophylline-binding RNA. *Biochemistry,* **37**, 9186-9192.